J. Phys. Chem. A **2008,** *112,* 849−857

Surprisingly Slow Reaction of Dimethylsilylene with Dimethylgermane: Time-Resolved Kinetic Studies and Related Quantum Chemical Calculations

Rosa Becerra

Instituto de Quimica-Fisica "Rocasolano", C.S.I.C., C/Serrano 119, 28006 Madrid, Spain

Sergey E. Boganov, Mikhail P. Egorov, Valery I. Faustov, Irina V. Krylova, Oleg M. Nefedov, and Vladimir M. Promyslov

N.D. Zelinsky Institute of Organic Chemistry, Russian Academy of Sciences, Leninsky Prospekt 47, 119991 Moscow, Russian Federation

Robin Walsh*

Department of Chemistry, University of Reading, Whiteknights, P. O. Box 224, Reading RG6 6AD, U.K.

Received: November 9, 2007

Time-resolved studies of silylene, SiH_2, and dimethylsilylene, $SiMe_2$, generated by the 193 nm laser flash photolysis of appropriate precursor molecules have been carried out to obtain rate constants for their bimolecular reactions with dimethylgermane, Me_2GeH_2, in the gas phase. $SiMe_2 + Me_2GeH_2$ was studied at five temperatures in the range 299−555 K. Problems of substrate UV absorption at 193 nm at temperatures above 400 K meant that only three temperatures could be used reliably for rate constant measurement. These rate constants gave the Arrhenius parameters $\log(A/\text{cm}^3\ \text{molecule}^{-1}\ \text{s}^{-1}) = -13.25 \pm 0.16$ and $E_a = -(5.01 \pm 1.01)$ kJ mol^{-1}. Only room temperature studies of SiH_2 were carried out. These gave values of $(4.05 \pm 0.06) \times 10^{-10}$ cm^3 molecule^{-1} s^{-1} ($SiH_2 + Me_2GeH_2$ at 295 K) and also $(4.41 \pm 0.07) \times 10^{-10}$ cm^3 molecule^{-1} s^{-1} ($SiH_2 + MeGeH_3$ at 296 K). Rate constant comparisons show the surprising result that $SiMe_2$ reacts 12.5 times slower with Me_2GeH_2 than with Me_2SiH_2. Quantum chemical calculations (G2(MP2,SVP)//B3LYP level) of the model Si−H and Ge−H insertion processes of $SiMe_2$ with SiH_4/$MeSiH_3$ and GeH_4/$MeGeH_3$ support these findings and show that the lower reactivity of $SiMe_2$ with Ge−H bonds is caused by a higher secondary barrier for rearrangement of the initially formed complexes. Full details of the structures of intermediate complexes and the discussion of their stabilities are given in the paper. Other, related, comparisons of silylene reactivity are also presented.

Introduction

Studies of the so-called "heavy carbenes", MR_2, where M = Si, Ge and R = H, Me are of fundamental interest because of the ubiquitous involvement of these intermediates in the breakdown mechanisms of organosilicon and organogermanium compounds.[1,2] Moreover, the particular prototype species, SiH_2 and GeH_2, are important in the mechanisms of chemical vapor deposition (CVD) leading to formation of electronic device materials.[3,4]

Gas-phase kinetic studies of silylenes[5−7] have shown that $SiMe_2$ is significantly less reactive than SiH_2. For example, at 298 K, rate constants for the Si−H insertion reactions of $SiMe_2$ (with the methylsilanes), are in the range $(0.2-5.5) \times 10^{-12}$ cm^3 molecule^{-1} s^{-1},[8] while those for SiH_2 lie in the range $(2.5-4.0) \times 10^{-10}$ cm^3 molecule^{-1} s^{-1}.[9−11] Even more striking effects have been found with germylenes. Recent gas-phase kinetic studies[12] have shown that $GeMe_2$ is at least a factor of 21 300 less reactive than GeH_2 with Me_2GeH_2 at 298 K. These decreases in reactivity have been attributed to the electron-withdrawing effect of the methyl groups in the silylene[5,6] and germylene.[12] This idea has drawn support from quantum chemical calculations which indicate that these reactions proceed via intermediate complexes whose stabilities are drastically reduced when Me-for-H substitution takes place on the silylene or germylene portion of the complex.[12]

Up to now, rate constant comparisons between silylene and germylene insertion reactions have been largely confined to SiH_2-with-silane and GeH_2-with-germane reactions.[7,12−14] The few exceptions to this include $SiH_2 + GeH_4$,[15] $GeH_2 + SiH_4$,[16] and $GeH_2 + Me_3SiH$.[17] Only with studies of these mixed Si/Ge reaction systems is it possible to make comparisons of the reactivities of different heavy carbenes with the same substrate (reaction partner) or of a particular heavy carbene with two substrates containing different group 14 elements. Such an exercise is useful because it allows a test of a long-held tenet of chemical reactivity, viz., that for any reactive intermediate rates should be faster with substrates with weaker bonds.[18] [Although there are various versions of this idea, one of the earliest is attributed to Evans−Polanyi,[18] who noted the correlation between activation energies and overall exothermicities (ΔH) for homologous series of abstraction reactions.] The evidence from the studies so far is ambiguous. Thus $GeH_2 + SiH_4$ ($k = 1.3 \times 10^{-11}$ cm^3 molecule^{-1} s^{-1} [16]) is slower than $GeH_2 + GeH_4$ ($k = 5.5 \times 10^{-11}$ cm^3 molecule^{-1} s^{-1} [19]) as expected (Si−H bonds are stronger than Ge−H bonds), but by

* To whom correspondence should be addressed.

10.1021/jp710740a CCC: $40.75 © 2008 American Chemical Society
Published on Web 01/15/2008

contrast, $SiH_2 + GeH_4$ ($k = 3.1 \times 10^{-10}$ cm^3 molecule^{-1} s^{-1}[15]) is slower than $SiH_2 + SiH_4$ ($k = 4.6 \times 10^{-10}$ cm^3 molecule^{-1} s^{-1}[10]), which is not expected. The third reaction, viz., $GeH_2 + Me_3SiH$ ($k = 8.2 \times 10^{-11}$ cm^3 molecule^{-1} s^{-1}[17]), is slower than $GeH_2 + Et_3GeH$ ($k = 2.7 \times 10^{-10}$ cm^3 molecule^{-1} s^{-1}[14]), as one might expect, but this assumes that Et− and Me− substituents are equivalent and we have recently found[12,14] that this is not the case (Et− is more activating than Me−). Rather more striking is the behavior of ClSiH, where reactions with $MeGeH_3$ and Me_2GeH_2 are almost 5 times slower than reactions with $MeSiH_3$ and Me_2SiH_2,[20] once again the unexpected result. In order to investigate this question further, we decided to study the reaction of $SiMe_2$ with Me_2GeH_2 (reaction 6). This will permit a comparison with the reaction $SiMe_2 + Me_2SiH_2$.[8] This latter reaction is the fastest Si−H insertion reaction of $SiMe_2$ among the methylsilanes and therefore suggests that (6) might be the fastest reaction of $SiMe_2$ with the methylgermanes. Reaction 6 will also provide a comparison with the recently studied and exceptionally slow reaction of $GeMe_2$ with Me_2GeH_2.[12] In order to provide further comparisons, more limited studies (room temperature only) have been carried out on $SiH_2 + MeGeH_3$ (reaction 2) and $SiH_2 + Me_2GeH_2$ (reaction 3). There have been no previous gas-phase experimental studies of these reactions.

In addition we have undertaken quantum chemical (ab initio) studies of the reactions ((4) and (5)) of $SiMe_2$ with GeH_4 and $MeGeH_3$ and the analogous reactions ((7) and (8)) of $SiMe_2$ with SiH_4 and $MeSiH_3$, in order to obtain information about the potential energy surfaces of these processes and thereby gain further insight into the mechanistic differences between reactions of $SiMe_2$ with germanes and silanes. Previously Sakai and Nakamura (SN)[21] have calculated barriers of 41 and 46 kJ mol^{-1} for reactions 7 and 8, respectively, at the MP4/6-31G(d,p)//MP2/6-31G(d,p) and MP3/6-31G(d,p)//MP2/3-21G(d) levels, respectively. Also, Su[22] has calculated energy barriers of 6 and 26 kJ mol^{-1} for reactions 4 and 7, respectively, at the CCSD(T) level using B3LYP optimized structures.

Except for (1) the reactions investigated here, either experimentally or theoretically, are

$$SiH_2 + GeH_4 \rightarrow H_3SiGeH_3 \quad (1)$$

$$SiH_2 + MeGeH_3 \rightarrow H_3SiGeH_2Me \quad (2)$$

$$SiH_2 + Me_2GeH_2 \rightarrow H_3SiGeHMe_2 \quad (3)$$

$$SiMe_2 + GeH_4 \rightarrow HMe_2SiGeH_3 \quad (4)$$

$$SiMe_2 + MeGeH_3 \rightarrow HMe_2SiGeH_2Me \quad (5)$$

$$SiMe_2 + Me_2GeH_2 \rightarrow HMe_2SiGeHMe_2 \quad (6)$$

$$SiMe_2 + SiH_4 \rightarrow HMe_2SiSiH_3 \quad (7)$$

$$SiMe_2 + MeSiH_3 \rightarrow HMe_2SiSiH_2Me \quad (8)$$

Experimental Section

Rate Measurements. Silylene kinetic studies have been carried out by the laser flash photolysis/laser absorption technique, details of which have been published previously.[8,10,23,24] Only essential and brief details are therefore included here. Silylenes were produced by the 193 nm flash photolysis of gaseous mixtures containing suitable precursors using a Lambda Physik (Coherent) Compex 100 exciplex laser, operating with ArF. Photolysis pulses were fired, at right angles, into a variable temperature reaction Spectrosil quartz vessel with demountable windows which were regularly cleaned. Photolysis pulse energies were typically 60−80 mJ with a variation of ±5%. The monitoring laser beam was multipassed 36 times along the vessel axis, through the reaction zone, to give an effective path length of 1.4 m. A portion of the monitoring beam was split off before entering the vessel for reference purposes. Light signals were measured by a dual photodiode/differential amplifier combination, and signal decays were stored in a transient recorder (Datalab DL910) interfaced to a BBC microcomputer. This was used to average the decays of up to five photolysis laser shots (at a repetition rate of 1 or 0.5 Hz). The averaged decay traces were processed by fitting the data to an exponential form using a nonlinear least-squares package. This analysis provided the values for first-order rate coefficients, k_{obs}, for removal of SiH_2 and $SiMe_2$ in the presence of known partial pressures of substrate.

The photoprecursors for the silylenes were silacyclopent-3-ene (SCP) for SiH_2 and 1,1-dimethyl-1-silacyclopent-3-ene (DMSCP) for $SiMe_2$. The monitoring lasers were a CW argon ion laser (Coherent Innova 90-5), for $SiMe_2$, and a single mode dye laser (Coherent 699-21) pumped by the Ar ion laser, for SiH_2. Both silylenes were detected via absorption in their strong $\tilde{A}(^1B_1) \leftarrow \tilde{X}(^1A_1)$ absorption bands, $SiMe_2$ at 457.9 nm[23] and SiH_2 at 579.39 nm (17 259.50 cm^{-1}), a strong vibration−rotation transition.[24,25] The dye laser wavelength was set by the combined use of a wave meter (Burleigh WA-20) and reference to a known coincident transition in the visible spectrum of I_2 vapor and was checked at frequent intervals during the experiments.

Gas mixtures for photolysis were made up containing a small pressure of precursor (SCP, 2.5 mTorr; DMSCP, 20−50 mTorr) and varying pressures of substrate (up to 20 mTorr for the SiH_2 studies; up to 40 Torr for the $SiMe_2$ studies). For the SiH_2 studies, inert diluent, SF_6, was also added to give total pressures of 10 Torr. All gases used in this work were frozen and rigorously pumped to remove any residual air prior to use.

$MeGeH_3$ and Me_2GeH_2 were synthesized by literature methods described previously.[12] SCP was prepared by the reduction of 1,1-dichloro-1-silacyclopent-3-ene with $LiAlH_4$ in ether in 60% yield following literature procedures.[26] 1,1-Dichloro-1-silacyclopentene-3 was obtained from *cis*-1-chloro-4-trichlorosilylbut-2-ene and Mg in 58% yield and the latter compound was prepared by reaction of *cis*-1,4-dichlorobut-2-ene and trichlorosilane in 50% yield, both following published procedures.[26] DMSCP was prepared by reaction of 1,1-dichloro-1-silacyclopent-3-ene with MeMgBr in 70% yield, again according to published procedures.[27] SCP and DMSCP were purified by low-pressure distillation to greater than 90%. All compounds were checked for purity by GC analysis (2 m silicone column, OV101) using a Perkin-Elmer 8310 chromatograph operated at ambient temperature. Purities were for $MeGeH_3$, 99.3%; for Me_2GeH_2, $>$99.5%; for SCP, 99%; and for 1,1-DMGCP, 91%. The small impurity in $MeGeH_3$ was Me_2GeH_2. The small impurities in Me_2GeH_2 were $MeGeH_3$ and Me_3GeH. SF_6 (no GC-detectable impurities) was from Cambrian Gases.

Density Functional Theory (DFT) and ab Initio Calculations. The DFT calculations, including the finding and verification of stationary points, were done with the B3LYP functional[28] using the 6-31G(d) basis.[29] All the structures obtained here were verified, by examination of their Hessian matrix, as minima (all frequencies real) or transition states (one imaginary frequency). The identities of transition states to particular reactions were established by B3LYP calculations along the minimum energy

paths (intrinsic reaction coordinate, IRC) connecting them with local minima. Electronic energies were corrected to include zero point vibrational energy (ZPE) contributions. For this purpose we used the scaling factor of 0.9806 recommended for B3LYP frequencies.[30] For all stationary points, enthalpies at 298 K were also calculated using harmonic oscillator and rigid rotor models.

Ab initio G2(MP2,SVP)[31] energy calculations were done for all minimal energy species on the potential energy surfaces of reactions studied. As we used geometries and frequencies obtained at the B3LYP/6-31G(d) level, we denote this type of calculation as G2(MP2,SVP)//B3LYP or simply G2MP2B3 for short. The same computational scheme was previously used in our studies of germylene reactions,[32,33] where it was shown to give results which were very close to those obtained with the standard version[34] of G2 theory.

Most of the calculations carried out here were performed using Gaussian 98[35] at the computer center of IOC RAS, Moscow.

Results

General Considerations. Previous measurements[12] of the UV spectra of $MeGeH_3$ and Me_2GeH_2 gave 193 nm absorption cross section values of 5.9×10^{-21} and 4.2×10^{-21} cm^2, respectively, at room temperature. These are very low values and under experimental conditions indicate very little absorption of the excimer laser beam at 298 K. However, it was also found earlier[12] that 193 nm photolysis of Me_2GeH_2 at temperatures above 398 K produces a transient species, so it seems likely that Me_2GeH_2 has a stronger absorption at higher temperatures, probably due to peak broadening.

For each reaction of interest it was independently verified during preliminary experiments that, in a given reaction mixture, k_{obs} values were not dependent on the exciplex laser energy or number of photolysis shots. Because static gas mixtures were used, tests with up to 15 shots were carried out. The constancy of k_{obs} (five shot averages) showed no effective depletion of reactants in any of the systems. The sensitivity of detection of $SiMe_2$ was high but decreased with increasing temperature. Therefore increasing quantities of precursor were required at higher temperatures. However, at any given temperature precursor pressures were kept fixed to ensure a constant (but always small) contribution to k_{obs} values.

For the $SiMe_2 + Me_2GeH_2$ studies, a series of experiments was carried out at five temperatures in the range from room temperature up to ca. 555 K. In these experiments, a number of runs (ca. five) at different Me_2GeH_2 partial pressures (up to 40 Torr) were carried out at each temperature. The purpose of these experiments was to establish the second-order nature of the kinetics. However, the results were complicated by the finding (noted above[12]) that, at the higher temperatures, a reactive transient was produced from Me_2GeH_2 *alone*. This transient decayed at rates lower than those with $SiMe_2$ precursor present, but which varied with temperature and pressure of Me_2GeH_2.

For the SiH_2 studies, only carried out at ambient temperature, much lower pressures of substrate (Me_2GeH_2 or $MeGeH_3$) were needed and SF_6 was added up to a total pressure of 10 Torr. No experiments were undertaken at different total pressures.

Kinetics of $SiMe_2 + Me_2GeH_2$. This reaction was investigated over the temperature range 299−555 K. The second-order rate plots are shown in Figure 1 for the five temperatures studied. It should be noted that total pressures (essentially those of Me_2GeH_2) vary from run to run. Leaving aside the question of the nature of the absorbing transient at higher temperatures (but see below), it can be seen that reasonably linear plots resulted

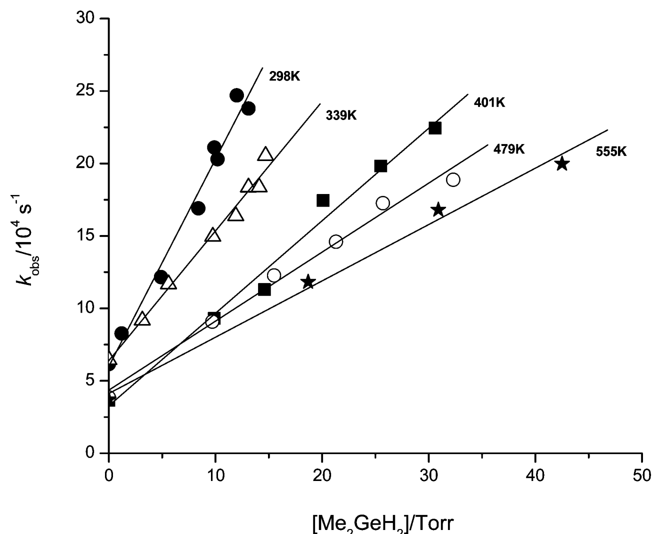

Figure 1. Second-order plots for reaction of $SiMe_2 + Me_2GeH_2$ at different temperatures (indicated).

TABLE 1: Experimental Second-Order Rate Constants[a] for $SiMe_2 + Me_2GeH_2$

T/K	$k_6/10^{-13}$ cm^3 molecule^{-1} s^{-1}
298.7	4.40 ± 0.23
339.4	3.14 ± 0.18
400.9	2.62 ± 0.13
479.4	2.40 ± 0.10[a]
555.0	2.27 ± 0.10[a]

[a] Values at 479.4 and 555.0 K are too high (see text)

and the second-order rate constants, obtained by least-squares fitting, are collected in Table 1. The error limits quoted are single standard deviations, but to allow for the possibility of other systematic sources of error, we estimate more realistic uncertainties of ±10%. The rate constants decrease with increasing temperature, but an Arrhenius plot of k_6 values, shown in Figure 2, clearly shows signs of curvature beyond experimental uncertainty. Because of the strong likelihood (see below) that decays at 479 and 555 K are disturbed by the presence of another absorbing intermediate, Arrhenius lines are shown only for the data obtained at the lower temperatures, either at 299 and 339 K (two-point line) or at 299, 339, and 401 K (three-point line). The following Arrhenius parameters were obtained.

two-point line: $$\log(k_6/\text{cm}^3\ \text{molecule}^{-1}\ \text{s}^{-1}) = -13.58 + 7.00\ \text{kJ mol}^{-1}/RT \ln 10$$

three-point line: $$\log(k_6/\text{cm}^3\ \text{molecule}^{-1}\ \text{s}^{-1}) = (-13.25 \pm 0.16) + (5.01 \pm 1.01)\ \text{kJ mol}^{-1}/RT \ln 10$$

Tests were made of the pseudo-first-order decays of the absorbing species produced from Me_2GeH_2 alone at 479 and 555 K. The decay constants were proportional to [Me_2GeH_2] and gave second-order rate constants (k/cm^3 molecule^{-1} s^{-1}) of 2.1×10^{-13} and 1.75×10^{-13}, respectively. Further details are reported in the Supporting Information. Because the signal intensity of this intermediate varied with Me_2GeH_2, it was not easy to make corrections for this in the presence of $SiMe_2$. In principle the presence of two absorbing intermediates should lead to double-exponential decays, but the relative closeness of the decay constants and the general system noise meant that data fitting to other than single-exponential decays was not

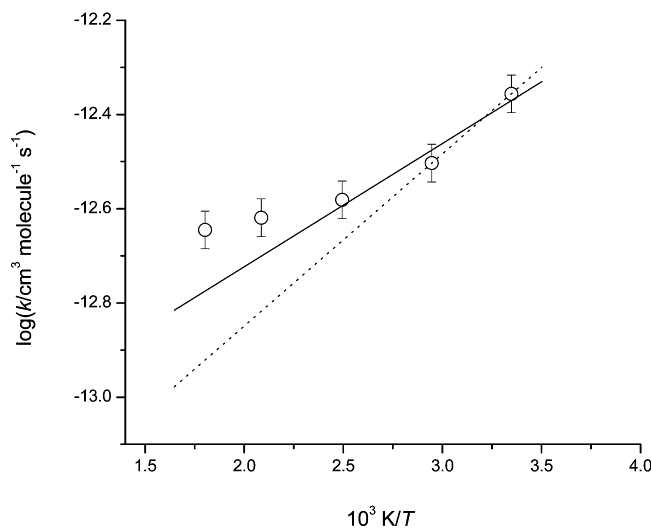

Figure 2. Arrhenius plot for rate constants for $SiMe_2 + Me_2GeH_2$ (○). —, fit for the *three* lower temperatures; ---, fit for the *two* lower temperatures.

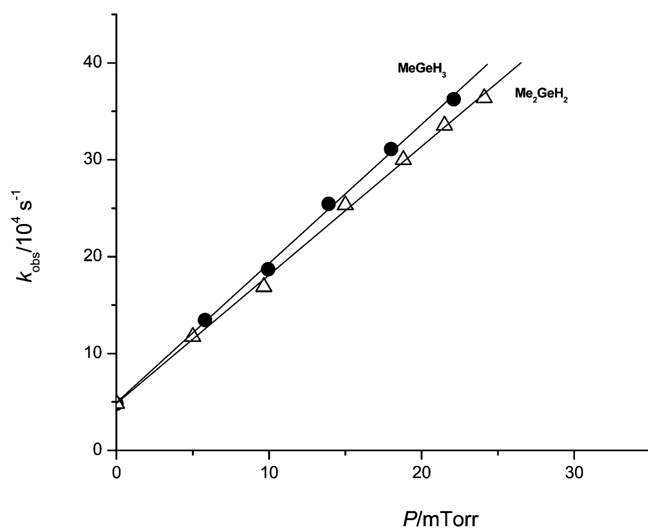

Figure 3. Second-order plot for reaction of SiH_2 at 10 Torr (SF_6) at 296 K with different substrates (indicated).

practicable. What is clearly the case is that at 479 and 555 K the apparent k_{obs} values include unknown contributions from another intermediate and therefore represent overestimates of the reaction rate constants for $SiMe_2$. At 299 and 339 K no absorptions could be detected from Me_2GeH_2 alone; at 401 K a small signal was seen barely beyond the noise level. It seems reasonable to assume that the lower three temperatures are unaffected by this problem, and therefore the Arrhenius parameters from the three-point fit should be reliable. While both two-point and three-point Arrhenius lines fit the data within experimental error, the three-point plot is preferable on statistical grounds.

Kinetics of $SiH_2 + MeGeH_3$. Only a room temperature (296 K) study of this reaction at a total pressure of 10 Torr (SF_6) has been carried out. The second-order rate plot is shown in Figure 3. This shows a good linear fit leading to a second-order rate constant of $(4.408 \pm 0.073) \times 10^{-10}$ cm^3 molecule^{-1} s^{-1}. No pressure or temperature variation studies of this reaction were undertaken.

Kinetics of $SiH_2 + Me_2GeH_2$. Only a room temperature (295 K) study of this reaction at a total pressure of 10 Torr (SF_6) has been carried out. The second-order rate plot is shown in Figure 3. This shows a good linear fit leading to a second-order rate constant of $(4.054 \pm 0.064) \times 10^{-10}$ cm^3 molecule^{-1} s^{-1}. No pressure or temperature variation studies of this reaction were undertaken.

Quantum Chemical Calculations. In order to provide a basis of comparison with experiment, which probes the effects of change of substrate from silane to germane and also the effects of methyl substitution in the substrate, we have undertaken G2MP2B3 calculations on reactions ((7) and (8)) of $SiMe_2$ with SiH_4 and $MeSiH_3$ and of the analogous reactions ((4) and (5)) of $SiMe_2$ with GeH_4 and $MeGeH_3$. The results of these calculations reveal a set of intermediate structures similar to those found in earlier theoretical calculations of silylene[10,11] and germylene[12,16,19] insertion reactions. Apart from the reactants and products, each reaction system indicates the presence of at least three stationary points and four in the case of reaction 7. In this latter case there are two local minima and two transition states, designated C1 and C2, and TS1 and TS2, respectively. For reactions 4, 5, and 8, C2 is missing. The local minima represent weakly bound H-bridged complexes with dimethylsilylene bridging the M−H bond (M = Si or Ge) into which insertion will take place in either a syn (C1) or anti (C2) configuration. The transition states TS1 and TS2 have the same configurations respectively as C1 and C2, and it is noteworthy that TS2 structures are found for all reactions, even though C2 complexes do not exist for three of them. This means that the pathways to particular disilane and silagermane products are not straightforward. For reactions 8 and 5 there is an additional complexity arising from the conformational possibilities for the Me group in the substrates $MeSiH_3$ and $MeGeH_3$. This can be either gauche or anti with respect to the migrating H-atom (C1) or skew-transoid or eclipsed with respect to the migrating H-atom (C2). These are labeled C1_1 and C1_2 (or C2_1 and C2_2), respectively. The same applies to the corresponding transition states. Note that for the purposes of this description it is assumed that C2 complexes exist in these cases. These details are summarized in the generic Figure 4. The individual pathways for each of the reactions investigated are shown in the topology diagram in Figure 5. Not shown in Figure 4 is the further complexity that the silylene−germane complexes (C1) show distortion from C_s or C_1 symmetry by dihedral rotations of the H_3Ge− or MeH_2Ge− groups around the Ge···Si axis. This means that these complexes have right- and left-handed forms and additional conformers. The angular distortions of these from C_s (or C_1) symmetry are generally small, with the largest being ca. 55°. Details of these rotational distortions are given in the Supporting Information, together with total energies and Cartesian coordinates of all stationary points.

The key geometric parameters for each of the complexes and transition states for all four reactions are given in Tables 2 and 3. A number of features of the data are worth pointing out. The complexes have long central bonds, Si···Si or Si···Ge, significantly longer than the bonds of the products (e.g., 2.357 Å for Si−Si in HMe_2SiSiH_3 and 2.382 Å for Si−Ge in HMe_2SiGeH_3). Si′···H* bonds are significantly longer than Si···H* in the Si−H insertion complexes (Si′ refers to the silicon atom from the silylene) and Si···H* are longer than the Ge···H* bonds in the Ge−H insertion complexes, indicating the rather small extent of H-atom transfer. Indeed, the Si···H* bond lengths show very little extension (<0.03 Å) compared with the calculated Si−H bond lengths of SiH_4 (1.486 Å) and $MeSiH_3$ (1.490 Å) and the Ge···H* bond lengths show little extension (<0.073 Å) compared with the calculated Ge−H bond lengths of GeH_4 (1.538 Å) and $MeGeH_3$ (1.546 Å). Change of substrate either from SiH_4 to $MeSiH_3$ or from GeH_4 to $MeGeH_3$ (i.e., Me-for-H

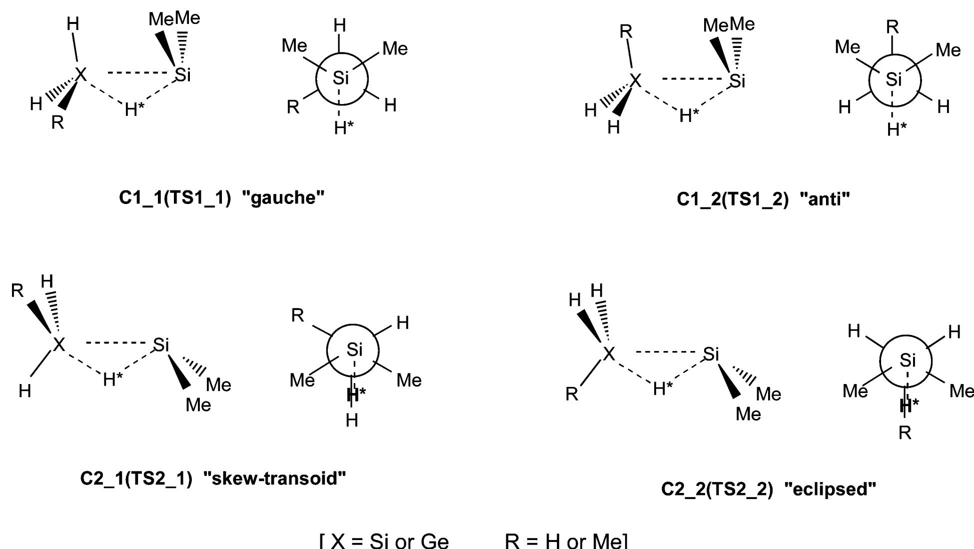

Figure 4. Generic structures of the complexes (local minima) and transition states found by B3LYP/6-31G(d) calculations for the reactions of $SiMe_2$ reactions with SiH_4/$MeSiH_3$ and GeH_4/$MeGeH_3$. Conformation names are based on the orientation of R (Newman projection) with respect to the migrating H-atom (marked with an asterisk).

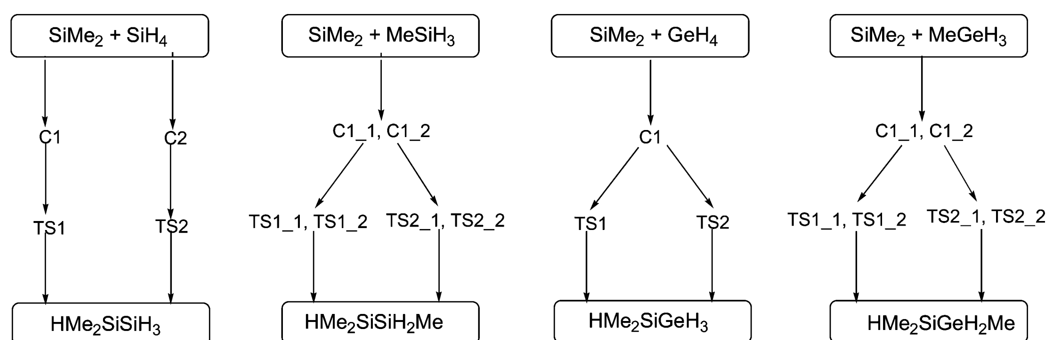

Figure 5. Topology diagram of the potential energy surfaces for the reactions of $SiMe_2$ with SiH_4, $MeSiH_3$, GeH_4, and $MeGeH_3$ from B3LYP/6-31G(d) calculations.

TABLE 2: Some Interatomic Distances[a] for Intermediates Formed in Reactions 7 and 8 Calculated at the B3LYP/6-31G(d) Level

reaction	species	bond length/Å		
		Si···Si′	Si···H*	Si′···H*
(7) $SiMe_2$+SiH_4	C1	3.552	1.508	2.154
	TS1	2.823	1.572	1.680
	C2	3.886	1.491	2.750
	TS2	2.483	1.623	1.765
(8) $SiMe_2$+$MeSiH_3$	C1_1	3.431	1.520	2.025
	TS1_1	2.656	1.869	1.537
	C1_2	3.518	1.517	2.056
	TS1_2	2.703	1.835	1.539
	C2_1			
	TS2_1	2.509	1.616	1.757
	C2_2			
	TS2_2	2.485	1.641	1.735

[a] To distinguish the Si atoms, that from the silylene is designated Si′.

TABLE 3: Some Interatomic Distances for Intermediates Formed in Reactions 4 and 5 Calculated at the B3LYP/6-31G(d) Level

reaction	species	bond length/Å		
		Ge···Si	Ge···H*	Si···H*
(4) $SiMe_2$+GeH_4	C1	3.151	1.608	1.836
	TS1	2.790	1.834	1.586
	C2			
	TS2	2.576	1.712	1.771
(5) $SiMe_2$+$MeGeH_3$	C1_1a[a]	3.184	1.612	1.817
	C1_1b[a]	3.143	1.619	1.799
	TS1_1	2.763	1.878	1.568
	C1_2	3.266	1.602	1.851
	TS1_2	2.802	1.872	1.564
	C2_1			
	TS2_1	2.595	1.712	1.738
	C2_2			
	TS2_2	2.601	1.722	1.753

[a] There are two gauche minima. See Supporting Information for structures.

substitution) produces only small geometrical effects on the complexes (≤0.129 Å for the Si−H insertion complexes; ≤0.115 Å for the Ge−H insertion complexes).

Geometry changes from complexes to transition states for each reaction pathway are as might be expected. For the Si−H insertion reactions there are significant reductions in Si···Si bond lengths by as much as 1.40 Å, increases in Si···H* by up to 0.35 Å, and reductions in Si′···H* by up to 0.99 Å. For the Ge−H insertions there are reductions in Si···Ge bond lengths by up to 0.67 Å, increases in Ge···H* by up to 0.27 Å, and reductions in Si···H* by up to 0.29 Å. These changes indicate a significant degree of H* transfer in all cases. The larger changes for the Si−H insertions reflect the fact that the complexes in these cases are rather looser. Change of substrate either from SiH_4 to $MeSiH_3$ or from GeH_4 to $MeGeH_3$ (i.e., Me-for-H substitution) produces generally small geometrical effects on the transition states (≤0.05 Å in the listed bond lengths) with the notable exception of those for TS1 for $SiMe_2$

TABLE 4: Electronic Energies (ΔE(0 K), Enthalpies (ΔH(298 K)), and Gibbs Free Energies (ΔG(298 K)) of Complexes,[a] Transition States,[a] and Products for Reactions 7, 8, 4, and 5 Calculated at the G2MP2B3 Level in kJ mol^{-1}

reactants	quantity	C1_1	C1_2	TS1_1	TS1_2	C2_1	C2_2	TS2_1	TS2_2	product
(7) $SiMe_2 + SiH_4$	ΔE(0 K)	−6, −3,[b] −5[c]		+17, +41,[b] +26[c]		−6		+1		−208, −204,[b] −216[c]
	ΔH(298 K)	−5		+14		−3		−4		−211
	ΔG(298 K)	+29		+63		+19		+47		−162
(8) $SiMe_2 + MeSiH_3$	ΔE(0 K)	−13	−12, −4[b]	+11	+16, +46[b]			−9	−6	−207, −204[b]
	ΔH(298 K)	−12	−11	+9	+14			−13	−10	−209
	ΔG(298 K)	+25	+24	+59	+61			+40	+42	−160
(4) $SiMe_2 + GeH_4$	ΔE(0 K)	−9, −3[c]		+2, +6[c]				+6		−223, −226[c]
	ΔH(298 K)	−11		−2				+2		−226
	ΔG(298 K)	+28		+41				+47		−184
(5) $SiMe_2 + MeGeH_3$	ΔE(0 K)	−17 (−16[d])	−15	−3	+1			−4	−1	−222
	ΔH(298 K)	−17 (−16[d])	−15	−5	−1			−7	−4	−224
	ΔG(298 K)	+25 (+25[d])	+26	+43	+48			+42	+45	−178

[a] For reactions 7 and 4, C1, TS1, C2, and TS2 have only one conformation. [b] Values from ref 21 calculated at the MP4/6-31G(d,p)//MP2/6-31G(d,p) level. [c] Values from ref 22 calculated at the CCSD(T)/LANL2DZdp//B3LYP/LANL2DZ level. [d] Value for alternative gauche conformation (this work).

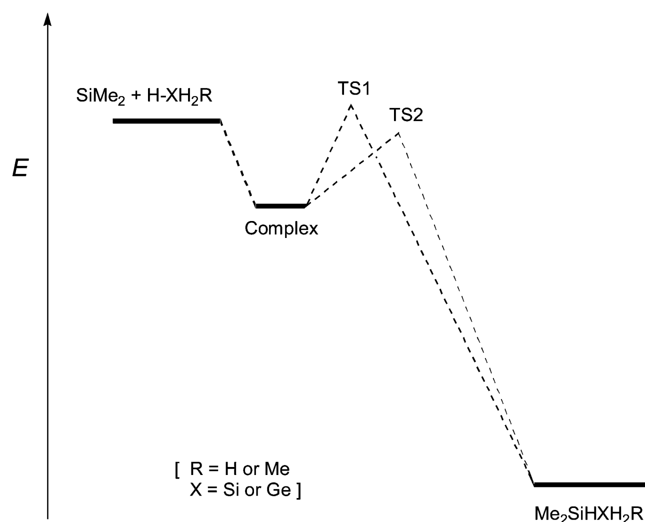

Figure 6. Generic potential energy surface for Si−H and Ge−H insertion reactions of $SiMe_2$.

+ $MeSiH_3$, where much larger changes particularly in the Si···H* bonds (up to 0.3 Å) were found.

The energies, enthalpies, and free energies associated with all the stationary point species are given in Table 4, and a generic potential energy surface is shown in Figure 6. A number of features can be discerned. The complexes (C1) for $SiMe_2$ with the germanes (reactions 4 and 5) are more stable than those with the silanes (reactions 7 and 8) in terms of ΔH, although ΔG values are very similar. With the exception of reaction 4 the transition states TS2 are lower in both ΔH and ΔG than TS1. Thus, although C2 complexes cannot generally be found, pathway 2 (from C1 to TS2) is generally favored over pathway 1 (from C1 to TS1). In the substrate, Me-for-H substitution stabilizes the complexes (C1) by 4−8 kJ mol^{-1} (ΔH) and lowers the enthalpies of the transition states by amounts up to 10 kJ mol^{-1}; in particular, the rate determining TS2 values are lowered by 6−10 kJ mol^{-1} (ΔG values are also lowered but by slightly less). The most interesting feature is that TS2 for reaction 8 lies lower in energy by 5−6 kJ mol^{-1} than TS2 for reaction 5. This indicates that reaction of $SiMe_2$ with $MeSiH_3$ should be favored over that with $MeGeH_3$. These observations apply whether we consider E(0 K), H(298 K), or G(298 K).

Because of the complexity of these calculations, we did not extend them to reactions 3 and 6.

Discussion

General Comments and Rate Constant Comparisons. The main experimental objective of the present study was to measure gas-phase rate constants for the reaction of $SiMe_2$ with Me_2GeH_2. This has been achieved at temperatures of 299, 339, and 401 K. At higher temperatures the complication of formation of a reactive intermediate from Me_2GeH_2 alone means that experimental decay constants in the reaction system of interest cannot be attributed solely to $SiMe_2$. Although the direct correction of decay traces was not possible, some idea of the overestimate of values of k_6 in Table 1 can be obtained by extrapolation of the Arrhenius plot of Figure 2. Based on the three lowest temperatures the calculated values of $k_6/10^{-13}$ cm^3 molecule^{-1} s^{-1} are 1.98 (479 K) and 1.66 (555 K). These are 83% and 73% of the measured decay constants at 479 and 555 K, respectively. If the Arrhenius line were steeper these percentages would be lower. Although the identity of the intermediate generated by the 193 nm photolysis of Me_2GeH_2 is unknown, it seems most likely to be methylgermylene, MeGeH. Its reactivity is clearly between those of GeH_2 and $GeMe_2$,[12] and its observed decay rate is consistent with the known kinetic behavior of MeGeH.[36]

There are no previous measurements of the absolute rate constants obtained in this study, although relative rates for reactions of SiH_2 with $MeGeH_3$ and Me_2GeH_2 have been reported by Sefcik and Ring at 623 K.[37] Considering first $SiMe_2$, we may immediately note that it is less reactive toward Me_2GeH_2 than toward Me_2SiH_2. The comparison of rate constants at room temperature is shown in Table 5, which also includes rate constant values for related reactions of ClSiH, which shows a similar pattern of relative reactivities, viz., ClSiH also reacts more slowly with germanes than with silanes. The possible reasons for this are considered later. The Arrhenius parameters for reaction 6 are compared with those for reactions of $SiMe_2$ with the methylsilanes in Table 6. The value of the A factor (A_6) for reaction of $SiMe_2$ with Me_2GeH_2 is fairly close to that for $SiMe_2 + Me_2SiH_2$, indicating that the main reason for the reactivity difference lies in the differing (negative) activation energies. Before discussing the origin of this, we consider the related kinetic data for SiH_2. Table 7 shows the comparison of room temperature rate constants for reactions of SiH_2 with the methylgermanes and methylsilanes. Here it is apparent that, whereas SiH_2 reacts more slowly with GeH_4 than with SiH_4, when it comes to the methyl derivatives the situation is reversed. This arises because Me-for-H replacement in the germane substrate series causes greater rate constant enhance-

TABLE 5: Some Rate Constant Comparisons for Ge−H and Si−H Insertion Reactions of $SiMe_2$ and ClSiH at Room Temperature

reaction	k_{Ge-H}[a]	reaction	k_{Si-H}[a]	k_{Ge-H}/k_{Si-H}
$SiMe_2 + Me_2GeH_2$	4.4×10^{-13} [b]	$SiMe_2 + Me_2SiH_2$	5.5×10^{-12} [c]	0.080
$ClSiH + MeGeH_3$	6.61×10^{-14} [d]	$ClSiH + MeSiH_3$	3.16×10^{-13} [d]	0.21
$ClSiH + Me_2GeH_2$	3.49×10^{-13} [d]	$ClSiH + Me_2SiH_2$	1.43×10^{-12} [d]	0.24

[a] Units: cm^3 $molecule^{-1}$ s^{-1}. [b] This work. [c] Reference 8. [d] Reference 20.

TABLE 6: Arrhenius Parameters for Ge−H and Si−H Insertion Reactions of $SiMe_2$

reaction	log(A/cm³ molecule⁻¹ s⁻¹)	E_a/kJ mol⁻¹	ref
$SiMe_2 + Me_2GeH_2$	−13.25	−5.01	this work
$SiMe_2 + SiH_4$	−12.54	+1.25	8
$SiMe_2 + MeSiH_3$	−12.90	−6.73	8
$SiMe_2 + Me_2SiH_2$	−13.15	−10.55	8
$SiMe_2 + Me_3SiH$	−13.41	−11.20	8

ments than in the silane series, on a per X−H basis (X = Ge or Si). This is shown in Table 8. It should, however, be borne in mind that the rate constants of Table 7 are all close to their collisional limits, and that the differences among them are not large. The data of Sefcik and Ring[37] apparently suggest that SiH_2 is ca. 32 times more reactive with Me_2GeH_2 than with $MeGeH_3$ at 623 K. This is considerably different from the value of 0.92 at 298 K which can be obtained from the figures of Table 8. However, the considerable differences in temperatures and pressures can explain this at least in part (see below).

We believe that the reactions studied here do not suffer from pressure dependence effects, and therefore true second-order rate constants have been obtained. In the main reaction of interest, viz., $SiMe_2 + Me_2GeH_2$, good second-order behavior was found although total pressures varied from run to run. In the SiH_2 reactions (2) and (3), there are three reasons to doubt such effects. First the products (H_3SiGeH_2Me, $H_3SiGeHMe_2$), even if formed initially vibrationally excited, are less likely to revert to reactants because they can decompose via the following alternative pathways.

$$H_3SiGeH_2Me^* \rightarrow SiH_4 + MeGeH$$

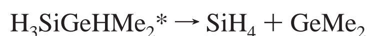

$$H_3SiGeHMe_2^* \rightarrow SiH_4 + GeMe_2$$

[For H_3SiGeH_3, formation of $SiH_4 + GeH_2$ is 92 kJ mol^{-1} more exothermic than $SiH_2 + GeH_4$[15]. $\Delta H°$ differences for these reactions should be similar.] This argument explains the lack of pressure dependence previously found[15] in reaction 1, $SiH_2 + GeH_4$.

Second, the analogous $SiH_2 + MeSiH_3$ and $SiH_2 + Me_2SiH_2$ reactions do not show pressure dependences at 298 K. Third, the values for k_2 and k_3 are essentially at their collisional limits and higher values would be unreasonable. These comments, however, do not apply to these reactions at 623 K, where pressure dependences are likely. Furthermore, in their study, Sefcik and Ring[37] used end product analysis to measure relative rates, and because of the alternative pathway decomposition it is likely that some part of the initial product

TABLE 8: Some Relative Rate Constants[a] for Ge−H and Si−H Insertion Reactions of SiH_2 at Room Temperature: Methyl Substituent Effect

reaction	k_{rel}	k_{rel}(per X−H)
$SiH_2 + GeH_4$	1[b]	1[b]
$SiH_2 + MeGeH_3$	1.44	1.92
$SiH_2 + Me_2GeH_2$	1.32	2.65
$SiH_2 + SiH_4$	1[c]	1[c]
$SiH_2 + MeSiH_3$	0.89	1.19
$SiH_2 + Me_2SiH_2$	0.76	1.52
$SiH_2 + Me_3SiH$	0.54	2.17

[a] Based on the rate constants of Table 7. [b] Reference reaction for Ge−H insertions. [c] Reference reaction for Si−H insertions.

was not stabilized. Thus the product ratios they obtained cannot be regarded as a true measure of the relative rate constants for insertion under their conditions.

Although we have not carried out product analytical studies, there is little doubt that the observed silylene reactions occur via Ge−H bond insertion. Lampe[38] has detected H_3SiGeH_3 in the reaction of $SiH_2 + GeH_4$. Sefcik and Ring[37] have observed the silylgermane products of the reactions of SiH_2 with the methylgermanes. Sakurai et al.[39] have observed the Ge−H insertion product of SiMePh (phenylmethylsilylene) with Et_3GeH. It is not expected that $SiMe_2$ should react differently from SiH_2 or SiMePh.

Further assistance in understanding these rate effects was obtained from the theoretical calculations discussed in the next section.

Quantum Chemical Calculations and the Barriers to Si−H and Ge−H Insertion Reactions. The results of our theoretical calculations indicate some differences from previous work. Both SN[21] and Su[22] found only one complex and one transition state for reaction 7, $SiMe_2 + SiH_4$ (corresponding to C1 and TS1). The geometries reported in both papers (see Supporting Information) show that the complexes were looser than those found by us for C1 and that the transition states showed a greater degree of H-atom transfer than ours in TS1. For the energies (Table 4, ΔE(0 K)/kJ mol^{-1}) the values for the complexes are similar to ours, but those for TS1, viz., 41[21] and 26,[22] are rather larger than ours of 17. However, the significant point is that both groups failed to find TS2, which is much lower in energy and therefore provides the actual reaction pathway transition state. Similar comments may be made about the calculations by SN[21] for reaction 8, $SiMe_2 + MeSiH_3$, although geometries found for C1 and TS1 were very similar to ours (see Supporting Information). For reaction 4, $SiMe_2 + GeH_4$, although Su[22] did not find a transition state corresponding to TS2, his energy values (Table 4) for C1 and TS1 are not very different from

TABLE 7: Some Rate Constant Comparisons for Ge−H and Si−H Insertion Reactions of SiH_2 at Room Temperature

reaction	k_{Ge-H}[a]	reaction	k_{Si-H}[a]	k_{Ge-H}/k_{Si-H}
$SiH_2 + GeH_4$	3.06×10^{-10} [b]	$SiH_2 + SiH_4$	4.60×10^{-10} [c]	0.67
$SiH_2 + MeGeH_3$	4.41×10^{-10} [d]	$SiH_2 + MeSiH_3$	4.10×10^{-10} [e]	1.08
$SiH_2 + Me_2GeH_2$	4.05×10^{-10} [d]	$SiH_2 + Me_2SiH_2$	3.50×10^{-10} [e]	1.16
$SiH_2 + Me_3GeH$		$SiH_2 + Me_3SiH$	2.54×10^{-10} [e]	

[a] Units: cm^3 $molecule^{-1}$ s^{-1}. [b] Reference 15. [c] Reference 10. [d] This work. [e] Reference 11.

ours. In fact, in this case because TS1 is slightly lower in energy than TS2, reaction via TS1 is probably the major pathway. The quantitative differences between our results and those of previous work,[21,22] apart from their failure to find alternative pathways, must be put down to the use of different levels of calculation and different basis sets.

As noted previously,[12,19] we believe that not too much significance should be attached to the complexity of rotational forms found here for some of the species. It is clear that both complexes and transition states are fairly mobile structures, and for a given species conformational energy differences are very small (3 kJ mol^{-1} at most). However, the finding of conformational switching between complexes and transition states is a novel feature of the present systems. In our previous calculations involving both silylene[10,11] and germylene[12,16,19] insertion processes, the reaction topologies were "linear", viz., C1 complexes reacted via TS1 transition states and C2 complexes reacted via TS2 transition states.

One of the motivations for the present calculations was to see whether and to what extent they could offer supporting evidence for the kinetic results. The finding of weakly bound complexes is just such evidence, but is no longer particularly surprising. The existence of such complexes in heavy carbene reactions is now well established.[10−12,16,19] What is more informative are the trends in energy values (either E(0 K) or H(298 K)) found here, particularly of the transition states, TS1 and TS2. Two effects are of interest. The first is the lowering of energies produced by Me-for-H replacement in the substrate (i.e., on changing from SiH_4 to $MeSiH_3$ or from GeH_4 to $MeGeH_3$). This is clear and unambiguous, although it varies slightly according to reaction pair. For insertions into Si−H bonds these are ca. 1−6 kJ mol^{-1} (TS1) and 6−10 kJ mol^{-1} (TS2). For insertions into Ge−H bonds they are ca. 1−5 kJ mol^{-1} (TS1) and 6−10 kJ mol^{-1} (TS2). This can account for the observed rate coefficient increase[8] of reaction 8, $SiMe_2$ + $MeSiH_3$, compared with reaction 7, $SiMe_2$ + SiH_4, although from our results the high barriers associated with TS1 mean that reaction should be limited to passage via TS2. Despite the fact that the reactions have not been studied, we would expect $SiMe_2$ to react faster with $MeGeH_3$, reaction 5, than with GeH_4, reaction 4. Our results show clearly that this is the case for the analogous reaction pair for SiH_2. For $SiMe_2$, there is the complication that apparently the pathway should switch from reaction via TS1 (reaction 4) to reaction via TS2 (reaction 5), although the energies of TS1 and TS2 are so close for reaction 5 that undoubtedly reaction via both pathways should occur. The Me-for-H substituent effects calculated here are very similar to those found earlier for other Si−H[11] and Ge−H[12] insertion reactions.

The second effect is the switch from substrate silanes to substrate germanes, viz., from Si−H to Ge−H insertion processes. TS1 enthalpy values show significant decreases of ca. 15 kJ mol^{-1}, such that whereas the Si−H insertions have significant positive barriers, the Ge−H insertions do not. However, it is the TS2 values which are of more interest because they are lower and the reactions occur either completely or partially via this pathway. The TS2 enthalpy differences are ca. 5−6 kJ mol^{-1} lower for Si−H compared to Ge−H insertion. The reason for this is not clear to us, but we note that the similarity of the critical bond lengths in the TS2 structures (Tables 2 and 3) between the two cases. This means that the larger 4p orbitals of the Ge atom require more distortion than the 3p orbitals of the Si atom. Another comparison shown in Table 9 provides added support for this argument. This shows

TABLE 9: Comparison of Theoretical Values (G2MP2B3 Level) of ΔE(0 K)/kJ mol^{-1} for Ge−H Insertion Reactions of $GeMe_2$ and $SiMe_2$

reactants	C1	TS1	TS2	ref
$GeMe_2 + GeH_4$	−4	+28	+29	12
$GeMe_2 + MeGeH_3$	−12	+25	+19	12
$SiMe_2 + GeH_4$	−9	+2	+6	this work
$SiMe_2 + MeGeH_3$	−17	−3	−4	this work

the comparison of TS2 energy values calculated for analogous $GeMe_2$ insertion processes with those of $SiMe_2$. The $GeMe_2$ values are ca. 23 kJ mol^{-1} higher than their $SiMe_2$ counterparts. Obviously in the $GeMe_2$ insertion reactions with Ge−H bonds, distortions of two Ge atom 4p orbitals are required. We have used this argument previously to explain why, in reaction with H_2, GeH_2 has an activation barrier (ca. 50 kJ mol^{-1}) whereas SiH_2 does not.[40]

It remains to consider whether there are any quantitative differences between these calculations and the experimental results of $SiMe_2$ obtained here. The calculated Me-for-H substituent effects in the substrate mean that for reactions of $SiMe_2$ with Me_2SiH_2 and Me_2GeH_2 we can expect further barrier reductions compared with those calculated for the reactions with $MeSiH_3$ and $MeGeH_3$. Approximate estimates (TS2, ΔH(298 K)/kJ mol^{-1}) would be −22 for $SiMe_2$ + Me_2SiH_2 and −16 for $SiMe_2$ + Me_2GeH_2. From the kinetics of the complex mechanism, described in previous papers,[5,7,8] these values should correspond approximately to the measured negative activation energies for these reactions. The differences between theory and experiment (Table 6) are 11−12 kJ mol^{-1}. While these are larger than we might have hoped, there are probably enough uncertainties in experiment, kinetic analysis, and theory to accommodate such differences. The trend in ΔG values (Me-for-H replacement) is slightly less than that in ΔH, indicating that activation entropies compensate somewhat. This helps reduce differences from experiment, but we do not believe a more elaborate kinetic analysis would eliminate them. The important point, however, is that the theory does predict more negative activation energies for the Si−H insertion than for the Ge−H insertion process.

The kinetic data for Ge−H and Si−H reactions of SiH_2 (Table 7) suggest that these arguments do not appear to apply to SiH_2. However, all published calculations for the Si−H insertion reactions of SiH_2[10,11] show that secondary barriers are very low, and offer no hindrance to reaction. Secondary barriers could well be higher for Ge−H insertions and still be low enough to exert rather little effect on rate constant values. The most likely reaction where an effect would show up is the reaction of SiH_2 + GeH_4, the one case where Ge−H insertion is actually slower than the analogous Si−H insertion. Unpublished calculations support this case.[41] For the methyl-substituted substrates, Me-for-H replacement almost certainly reduces the secondary barriers to even smaller values where any effect is even less. The greater k_{rel}(per X−H) values of Table 8 for the Ge−H insertions than for the Si−H insertions is in agreement with the idea that there is a small but nonzero effect of secondary barrier operating in the Ge−H insertion case.

From these studies it seems that to obtain significant inversion of relative rates for Ge−H compared with Si−H insertion reactions requires a stabilized silylene. $SiMe_2$ is known to be more stabilized in terms of its divalent state stabilization energy (DSSE) than SiH_2.[42] The origin of this is thought to be inductive electron withdrawal by the more electronegative Me groups. ClSiH is another such case where relative rate constant values disfavor Ge−H insertion (Table 5). In this case the ClSiH gains

its stabilization via back-donation of electron density from a Cl atom lone pair to the Si atom empty p orbital. Unpublished calculations also support these arguments.[43]

Some Further Enthalpy Considerations. *(a) Thermochemistry of Disilanes.* The theoretically calculated $\Delta H°(298\ K)$ values for reactions 7 and 8 may be compared with values of -220.9 and -215.9 kJ mol^{-1} obtained by use of the Allen bond additivity scheme based on the calorimetric value of $\Delta H_f°(Si_2Me_6)$.[44] These values have an estimated maximum uncertainty of ± 9 kJ mol^{-1}, which means that the calculated values of -211 and -209 kJ mol^{-1} (Table 4) are essentially in agreement.

(b) Thermochemistry of Silylgermanes. The theoretically calculated $\Delta H°(298\ K)$ values for reactions 4 and 5 may be compared with $\Delta H°(298\ K) = -242 \pm 10$ kJ mol^{-1} obtained for reaction 1, $SiH_2 + GeH_4 \rightarrow H_3SiGeH_3$, from experimental $\Delta H_f°$ values.[15] The additivity considerations for methyldisilanes[44] suggest that the values of $\Delta H°$ for reactions 4 and 5 might be slightly less negative than this but probably not by more than 5 kJ mol^{-1}. This means that the calculated values of -226 and -224 kJ mol^{-1} (Table 4) are in reasonable agreement with expectations based on experiment.

Conclusion

The experimental kinetic studies carried out here have shown the surprising result that $SiMe_2$ inserts into the Ge−H bonds of Me_2GeH_2 more than an order of magnitude more slowly than into the Si−H bonds of Me_2SiH_2. Model theoretical quantum chemical calculations demonstrate that in the mechanisms of both Si−H and Ge−H insertion, which occur via intermediate H-bonded complexes, the complexes with germane substrates have higher secondary barriers to rearrangement to final products than those with silane substrates. It is thought that this arises because of increased orbital strain. This is consistent with the kinetic findings.

Acknowledgment. S.E.B, M.P.E, V.I.F., I.V.K., O.M.N and V.M.P thank RFBR (Project Nos. 07-03-00693 and 06-03-33010), the President of the Russian Federation (Presidential program for support of leading research schools, Grant NSh-6075.2006.03), and the Russian Academy of Sciences (Program OX-01). R.B. thanks the Ministerio de Educacion y Ciencia, for support under Project No. CTQ2006-10512/BQU.

Supporting Information Available: Details of second-order plots for the unknown intermediate, comparisons of computed geometries with those from previous work, conformations of the DFT calculated structures, Cartesian coordinates for all stationary points, and complete ref 35. This material is available free of charge via the Internet at http://pubs.acs.org.

References and Notes

(1) *The Chemistry of Organic Silicon Compounds*; Rappoport, Z., Apeloig, Y., Eds.; Wiley: Chichester, 1998; Vol. 2.

(2) *The Chemistry of Organic Germanium, Tin and Lead Compounds*; Patai, S., Ed.; Wiley: Chichester, 1995; Vol. 1.

(3) Jasinski, J. M.; Gates, S. M. *Acc. Chem. Res.* **1991**, *24*, 9.

(4) Isobe, C.; Cho, H.; Crowell, J. E. *Surf. Sci.* **1993**, *295*, 117.

(5) Becerra, R.; Walsh, R. Kinetics and Mechanisms of Silylene reactions: a Prototype for Gas-phase Acid/base Chemistry. In *Research in Chemical Kinetics*; Compton, R. G., Hancock, G., Eds.; Elsevier: Amsterdam, 1995; Vol. 3, Chapter 6, p 263.

(6) Jasinski, J. M.; Becerra, R.; Walsh, R. *Chem. Rev.* **1995**, *95*, 1203.

(7) Becerra, R.; Walsh, R. *Phys. Chem. Chem. Phys.* **2007**, *9*, 2817.

(8) Baggott, J. E.; Blitz, M. A.; Frey, H. M.; Walsh, R. *J. Am. Chem. Soc.* **1990**, *112*, 8337.

(9) Baggott, J. E.; Frey, H. M.; Lightfoot, P. D.; Walsh, R.; Watts, I. M. *J. Chem. Soc., Faraday Trans.* **1990**, *86*, 27.

(10) Becerra, R.; Frey, H. M.; Mason, B. P.; Walsh, R.; Gordon, M. S. *J. Chem. Soc., Faraday Trans.* **1995**, *91*, 2723.

(11) Becerra, R.; Carpenter, I. W.; Gordon, M. S.; Roskop, L.; Walsh, R. *Phys. Chem. Chem. Phys.* **2007**, *9*, 2121.

(12) Becerra, R.; Boganov, S. E.; Egorov, M. P.; Faustov, V. I.; Krylova, I. V.; Nefedov, O. M.; Promyslov, V. M.; Walsh, R. *Phys. Chem. Chem. Phys.* **2007**, *9*, 4395−4406.

(13) Boganov, S. E.; Egorov, M. P.; Faustov, V. I.; Krylova, I. V.; Nefedov, O. M.; Becerra, R.; Walsh, R. *Russ. Chem. Bull. Int. Ed.* **2005**, *54*, 483.

(14) Becerra, R.; Boganov, S. E.; Egorov, M. P.; Krylova, I. V.; Nefedov, O. M.; Walsh, R. *J. Phys. Chem. A* **2007**, *111*, 1434.

(15) Becerra, R.; Boganov, S. E.; Walsh, R. *J. Chem. Soc., Faraday Trans.* **1998**, *94*, 3569.

(16) Becerra, R.; Boganov, S. E.; Egorov, M. P.; Faustov, V. I.; Nefedov, O. M.; Walsh, R. *Phys. Chem. Chem. Phys.* **2001**, *3*, 184.

(17) Becerra, R.; Walsh, R. *Phys. Chem. Chem. Phys.* **1999**, *1*, 5301.

(18) Evans, M. G.; Polanyi, M. *Trans. Faraday Soc.* **1936**, *32*, 1933; *Trans. Faraday Soc.* **1938**, *34*, 22.

(19) Becerra, R.; Boganov, S. E.; Egorov, M. P.; Faustov, V. I.; Nefedov, O. M.; Walsh, R. *J. Am. Chem. Soc.* **1998**, *120*, 12657.

(20) Becerra, R.; Boganov, S. E.; Egorov, M. P.; Krylova, I. V.; Nefedov, O. M.; Walsh, R. *Chem. Phys. Lett.* **2005**, *413*, 194.

(21) Sakai, S.; Nakamura, M. *J. Phys. Chem.* **1993**, *97*, 4960.

(22) Su, M.-D. *Chem.*−*Eur. J.* **2004**, *10*, 6073.

(23) Baggott, J. E.; Blitz, M. A.; Frey, H. M.; Lightfoot, P. D.; Walsh, R. *Chem. Phys. Lett.* **1987**, *135*, 39.

(24) Baggott, J. E.; Frey, H. M.; King, K. D.; Lightfoot, P. D.; Walsh, R.; Watts, I. M. *J. Phys. Chem.* **1988**, *92*, 4025.

(25) Jasinski, J. M.; Chu, J. O. *J. Chem. Phys.* **1988**, *88*, 1678.

(26) Damrauer, R.; Simon, R.; Laporterie, A.; Manuel, G.; Tae Park, Y.; Weber, W. P. *J. Organomet. Chem.* **1990**, *391*, 7.

(27) Chernyshev, E. A.; Komalenkova, N. G.; Bashkirova, S. A.; Sokolov, V. V. *J. Gen. Chem. USSR (Engl. Transl.)* **1978**, *48*, 757; *Z. Obshch. Khim.* **1978**, *48*, 830.

(28) Becke, A. D. *J. Chem. Phys.* **1993**, *98*, 5648.

(29) Hehre, W. A.; Radom, L.; Pople, J. A. *Ab Initio Molecular Orbital Theory*; Wiley: New York, 1986.

(30) Scott, R. J.; Radom, L. *J. Phys. Chem.* **1996**, *100*, 16502.

(31) Curtiss, L. A.; Redfern, P. C.; Smith, B. J.; Radom, L. *J. Chem. Phys.* **1996**, *104*, 5148.

(32) Becerra, R.; Boganov, S. E.; Egorov, M. P.; Faustov, V. I.; Krylova, I. V.; Nefedov, O. M.; Promyslov, V. M.; Walsh, R. *Phys. Chem. Chem. Phys.* **2004**, *6*, 3370.

(33) Becerra, R.; Boganov, S. E.; Egorov, M. P.; Faustov, V. I.; Promyslov, V. M.; Nefedov, O. M.; Walsh, R. *Phys. Chem. Chem. Phys.* **2002**, *4*, 5079.

(34) Curtiss, L. A.; Raghavachari, K.; Trucks, G. W.; Pople, J. A. *J. Chem. Phys.* **1991**, *94*, 7221.

(35) Frisch, M. J.; et al. *Gaussian 98*, revision A7; Gaussian, Inc.: Pittsburgh, PA, 1998.

(36) Becerra, R.; Harrington, C. R.; Leigh, W. J.; Kefala, L. A.; Walsh, R. *Organometallics* **2006**, *25*, 4439.

(37) (a) Sefcik, M. D.; Ring, M. A. *J. Am. Chem. Soc.* **1973**, *95*, 5168. (b) Sefcik, M. D.; Ring, M. A. *J. Organomet. Chem.* **1973**, *59*, 167.

(38) Lampe, F. W. *Spectrochim. Acta* **1987**, *43A*, 257.

(39) Sakurai, H.; Kobayashi, Y.; Nakadaira, Y. *J. Organomet. Chem.* **1976**, *120*, C1.

(40) Becerra, R.; Boganov, S. E.; Egorov, M. P.; Faustov, V. I.; Nefedov, O. M.; Walsh, R. *Can. J. Chem.* **2000**, *78*, 1428.

(41) Faustov, V. I.; Promyslov, V. M. Unpublished calculations.

(42) Becerra, R.; Walsh, R. Thermochemistry. In *The Chemistry of Organosilicon Compounds*; Rappoport, Z., Apeloig, Y., Eds.; John Wiley & Sons: New York, 1998; Vol. 2, Chapter 4, p 153.

(43) Faustov, V. I.; Promyslov, V. M. Unpublished calculations.

(44) Pilcher, G.; Leitão, M. L. P.; Yang, M.-Y.; Walsh, R. *J. Chem. Soc., Faraday Trans.* **1991**, *87*, 841.